

# Osteology of *Turfanodon bogdaensis* (Dicynodontia)

SHI Yu-Tai<sup>1,2</sup> LIU Jun<sup>1,2\*</sup>

(1 Key Laboratory of Vertebrate Evolution and Human Origins of Chinese Academy of Sciences, Institute of Vertebrate Paleontology and Paleoanthropology, Chinese Academy of Sciences Beijing 100044)

(2 College of Earth and Planetary Sciences, University of Chinese Academy of Sciences Beijing 100049)

\* Corresponding author: liujun@ivpp.ac.cn

**Abstract** Within the dicynodont genus *Turfanodon*, there are two recognized species, *T. bogdaensis* and *T. jiufengensis*. Both species are known by relatively complete cranial materials, but the mandibles and most postcranial bones have been described only for *T. jiufengensis*. This paper reports new dicynodont specimens from Turpan, Xinjiang, referring them to *T. bogdaensis*. They can clearly be differentiated from *T. jiufengensis* by the flatter lateral surface of the snout region, a prominent swelling on the lateral dentary shelf, and the rounded femoral head. The diagnosis of *Turfanodon* is revised. The combination of a flat circumorbital rim, posterior portion of anterior pterygoid rami with converging ventral ridges, and a possible autapomorphy, a deep notch on scapula forming procoracoid foramen, are confirmed. It also differentiated from all dicynodonts other than *Myosaurus*, *Kembawacela* and *Lystrosaurus* by having accessory ridges lateral to the median palatal ridge.

**Key words** Turpan, Xinjiang; Lopingian, Permian; Guodikeng Formation; Dicynodontia, *Turfanodon*; osteology, postcranial skeleton

**Citation** Shi Y T, Liu J, in press. Osteology of *Turfanodon bogdaensis* (Dicynodontia). *Vertebrata Palasiatica*. DOI: 10.19615/j.cnki.2096-9899.240529

## 1 Introduction

*Turfanodon* is a large-sized dicynodont of the late Permian Period. It was one of the most widely distributed dicynodonts in eastern Pangea and crossed both tropical and temperate zones (Sun, 1973; Li et al., 2000; Liu, 2021). The holotype of *T. bogdaensis* (IVPP V3241) was collected from the Guodikeng Formation of Turpan, Xinjiang, China. This genus was proposed as a junior synonym of *Dicynodon* (King, 1988), but has more recently been revalidated (Kammerer et al., 2011). Two species, *Striodon magnus* from Jimusar (Sun, 1978), and *D. sunanensis* from Gansu (Li et al., 2000), have been proposed as junior synonyms of *T. bogdaensis* (Kammerer et al., 2011). Recently, a second species, *T. jiufengensis*, was named based on specimens from the Naobaogou Formation of Nei Mongol, China (Liu, 2021). Currently, this genus is the most abundant Permian dicynodont in China.

*Turfanodon jiufengensis* is known from five specimens including crania, mandibles, and relatively complete postcrania, whereas *T. bogdaensis* is only known from cranial materials. Here we report a few new specimens of *T. bogdaensis*, including many postcranial bones, from the Guodikeng Formation of Turpan, Xinjiang, China. They provide more anatomical information on this species.

**Institutional abbreviations** IGCAGS, Institute of Geology, Chinese Academy of Geological Sciences, Beijing, China; IVPP, Institute of Vertebrate Paleontology and Paleoanthropology, Chinese Academy of Sciences, Beijing, China; NHMUK, The Natural History Museum, London, England, UK; RC, Rubidge Collection, Wellwood, Graaff-Reinet, South Africa.

## 2 Geological setting, material and methods

The studied specimens were collected in 2012 from the Guodikeng Formation of the South Taodonggou locality, Turpan, Xinjiang. A partial archosauriform left hindlimb (IVPP V22764) was excavated with the dicynodonts at the same locality. This specimen was recently made the holotype of a new taxon, *Vigilosaurus gaochangensis*, and its host layer is estimated to be around 252.2 Ma (Angielczyk et al., 2022; Chen and Liu, 2022).

For the dicynodont materials, most bones belong to a nearly complete specimen, IVPP V31402; whereas a smaller humerus, a femur and some vertebrae show the presence of a second specimen, IVPP V31403.

The nomenclature of the angular follows Olroyd and Sidor (2022); and some interpretations of the structure of the postcranial skeleton follow Bishop and Pierce (2023a, b).

## 3 Systematic paleontology

**Anomodontia** Owen, 1860

**Dicynodontia** Owen, 1859

**Dicynodontioidea** Olson, 1944

***Turfanodon*** Sun, 1973

**Revised diagnosis** (expanded from Liu, 2021) Large dicynodontoid with a tall, steeply-sloping snout, long caniniform process, heavily pitted facial region, flat circumorbital rim, elongated and narrow intertemporal bar, posterior portion of anterior pterygoid rami with converging ventral ridges. Possible autapomorphy: deep notch on scapula forming procoracoid foramen.

Differentiated from all dicynodonts other than *Myosaurus*, *Kembawacela* and *Lystrosaurus* by having accessory ridges lateral to the median palatal ridge. Differentiated from all dicynodontoids other than *Dinanomodon* by a contact between the premaxilla and the frontal. Differentiated from *Dinanomodon* by having the anterior tip of the snout squared

off and nasal bosses present as anteroposteriorly elongated swellings near the posterodorsal margin of external nares.

### *Turfanodon bogdaensis* Sun, 1973

**Holotype** IVPP V3241, an incomplete skull.

**Referred specimens** IGCAGS V296, an incomplete skull (holotype of “*Dicynodon sunanensis*”); IVPP V31402, an incomplete skull, mandible, and most of the postcranial bones; IVPP V31403, a humerus, a femur, three dorsal vertebrae and the 3rd–5th sacral vertebrae.

**Revised diagnosis** A large Permian dicynodontoid with a thick lateral dentary shelf. Differentiated from its congener *T. jiufengensis* by weakly developed nasal bosses, a median snout groove on premaxilla, flat lateral snout surface, a contact between maxilla and nasal (separating lacrimal from septomaxilla), prefrontal anterior extension not extending anterior to lacrimal, parietal exposed on midline groove of intertemporal bar, and proximal articular surface of femur more rounded.

**Locality and horizon** Turpan, Xinjiang and Sunan, Gansu; Guodikeng Formation and Sunan Formation, Lopingian (Changhsingian), Permian.

**Description** The skull of IVPP V31402 is nearly complete except for the missing left postorbital bar, right zygomatic arch, and both caniniform processes (Fig. 1). The bone surfaces are poorly preserved, so many sutures and detailed features are hard to discern.

The premaxilla has an incomplete anterior margin (Fig. 1). The bone surface is strongly eroded, so neither a groove, as in IVPP V3241 and IGCAGS V296, nor a ridge, as in *Turfanodon jiufengensis*, can be observed. The premaxilla contacts the frontal posterodorsally, which is a diagnostic character of *Turfanodon* (Fig. 1B) (Sun, 1973; Liu, 2021). The premaxillary anterior surface is clearly demarcated from the lateral surfaces, and the lateral surface of the snout region is flat, not a bi-planar surface as in *T. jiufengensis*. In *T. jiufengensis*, the maxilla turns more laterally than the premaxillary lateral surface, forming a concave area below the external naris (Fig. 2A, B) (Liu, 2021). The snout is tall and sloping (Fig. 1E, F). Two faint accessory ridges lie lateral to the median palatal ridge, as *T. jiufengensis* (Fig. 1C, D) (Liu, 2021). This character has only been reported as present in *Myosaurus*, *Kembawacela* and *Lystrosaurus* previously (Cluver, 1971, 1974; Angielczyk et al., 2021a).

The septomaxilla forms a concavity posterior to the naris (Fig. 1E). Both caniniform processes are broken, so the preserved maxillary ventral margin lies above the level of the quadrate (Fig. 1E, F). The maxillary lateral surface is rather smooth, without the distinct buttress as in IVPP V3241, similar to IGCAGS V296 (Liu, 2021).

The nasals are separated from each other by the contact of the premaxilla with the frontal (Fig. 1B). The paired nasal bosses are weakly developed (Fig. 1E, F), as in IGCAGS V296, while they are hardly discernable in IVPP V3241. The nasal bosses of all of these specimens are less pronounced than those of *T. jiufengensis*.

The maxilla, the jugal and the squamosal contribute to the zygomatic arch. Laterally, the

jugal is covered by the maxilla anteriorly and the squamosal posteroventrally, and it is exposed as a narrow strip below the orbit. The jugal also extends dorsally to form part of the posterior edge of the postorbital bar (Fig. 1E, F). Ventrally, the jugal contributes to the subtemporal arch (Fig. 1C, D). It also forms the dorsolateral margin of the labial fossa (Fig. 1C–F).

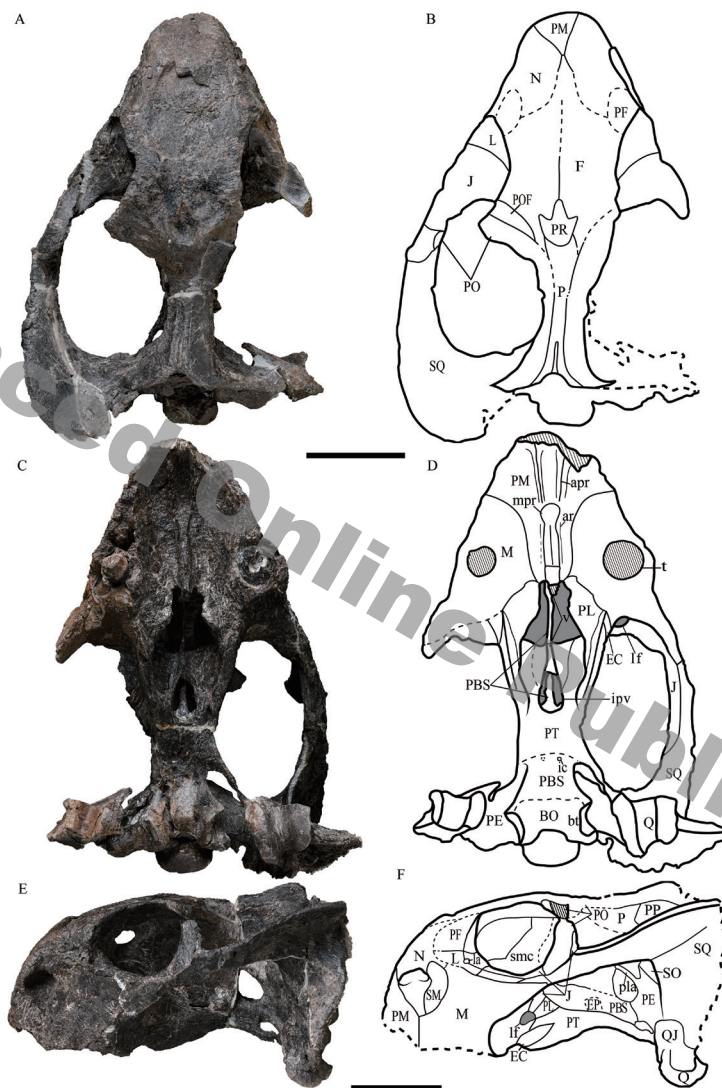


Fig. 1 *Turfanodon bogdaensis* (IVPP V31402) from the Guodikeng Formation, Turpan, Xinjiang

Photos and drawings of skull in dorsal (A, B), ventral (C, D) and lateral (E, F) views

Abbreviations: apr. anterior palatal ridge; ar. accessory ridge; BO. basioccipital; bt. basal tuber; EC. ectopterygoid; EP. epipterygoid; F. frontal; ic. internal carotid canal; ipv. interpterygoid vacuity; J. jugal; L. lacrimal; la. lacrimal fossa; lf. labial fossa; M. maxilla; mpr. median palatal ridge; N. nasal; P. parietal; PBS. parabasisphenoid; PE. periotic; PF. prefrontal; PL. palatine; pla. pila antotica; PM. premaxilla; PO. postorbital; POF. postfrontal; PP. postparietal; PR. preparietal; PT. pterygoid; Q. quadrate; QJ. quadratojugal; SM. septomaxilla; smc. sphenethmoid complex; SO. supraoccipital; SQ. squamosal; t. tusk; V. vomer. Scale bars equal 5 cm

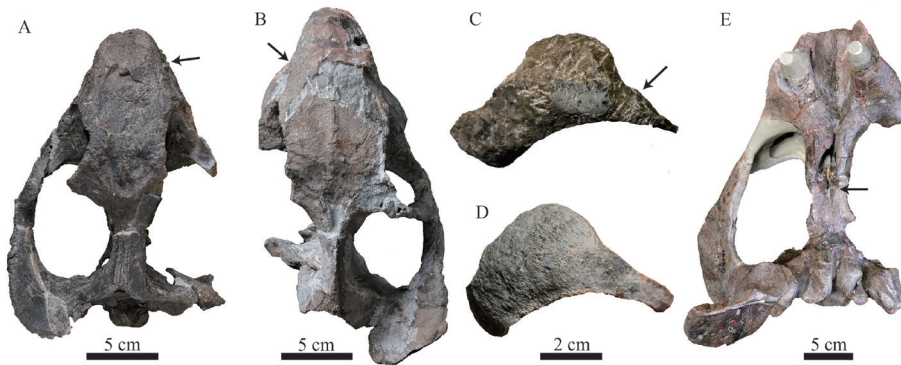


Fig. 2 The skulls and humerus of *Turfanodon* and the humerus of *Lystrosaurus*  
 A, B. the skulls of *T. bogdaensis*, IVPP V31402 (A) and *T. jiufengensis*, V26035 (B) in dorsal view, the arrows indicate the difference of snout region; C, D. comparison of left humerus of *T. bogdaensis*, V31402 (C) and mirrored right humerus of *Lystrosaurus* (D) in proximal view, the arrow indicates a bulge which is strongly developed in *T. bogdaensis*, it is the insertion of the *M. supracoracoideus* (supraspinatus);  
 E. the holotype (V3241) of *T. bogdaensis* in ventral view, the arrow indicates the trace of the keel of anterior pterygoid ramus

The zygomatic process of the squamosal tapers anteriorly as a narrow wedge, with a straight suture with the maxilla (Fig. 1E, F), same as in IVPP V3241 (Sun, 1973, Fig. 3) and IGCAGS V296. The same morphology may also be present in *T. jiufengensis*, although Liu (2021) explained the squamosal inserts in the jugal, and contacting with maxilla only on its posterior portion.

The fat prefrontal forms the anterodorsal corner of the orbit (Fig. 1). The bone surface is poorly preserved, so its suture with the lacrimal and its anterior extension are hard to trace.

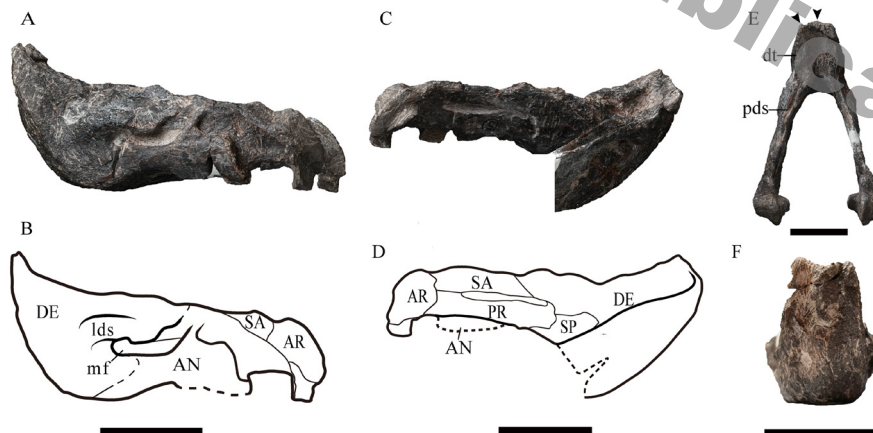


Fig. 3 *Turfanodon bogdaensis* (IVPP V31402) from the Guodikeng Formation, Turpan, Xinjiang  
 Mandible photos and drawings in left lateral (A, B), dorsolateral (C, D), dorsal (E) and anterior (F) views;  
 the arrow heads indicate the median and lateral ridges

Abbreviations: An. angular; Ar. articular; De. dentary; dt. dentary table; lds. lateral dentary shelf;  
 mf. mandibular fenestra; pds. posterior dentary sulcus; Pr. prearticular; Sa. surangular; SP. splenial  
 Scale bars equal 5 cm

Based on bone surface texture, it seems that those two bones extend anteriorly at the same level and the lacrimal does not touch the septomaxilla (Fig. 1E, F).

The frontal contacts the premaxilla anteriorly (Fig. 1B). The postfrontal is wedge-shaped, as in the holotype (Fig. 1B). The preparietal is depressed, showing the shape of a ‘three-toe’ footprint, with one large median process and two smaller lateral processes (Fig. 1A, B). This shape is similar to that of those relatively small specimens of *T. jiufengensis*, but differs from IVPP V3241 and IGCAGS V296 (Liu, 2021).

The intertemporal bar is formed by the postorbital and the parietal (Fig. 1A, B). The postorbital orients obliquely, slightly different from the other known specimens of *T. bogdaensis*. In the holotype, the postorbital is nearly vertical in this region, while in IGCAGS V296, the intertemporal bar has some deformation, but a vertical orientation can be recognized. *Turfanodon jiufengensis* has a vertically oriented postorbital, as in IVPP V3241. The parietal is bounded by the postorbitals laterally and has a narrow exposure on the dorsal surface. There is a shallow midline groove formed by the parietal posteriorly (Fig. 1A, B), unlike the crest-like exposure in *T. jiufengensis* (IVPP V26035) (Fig. 2). In both IVPP V3241 and IGCAGS V296, the parietal is exposed in the groove formed by the postorbitals (Liu, 2021). Overall, *T. bogdaensis* has a wider intertemporal bar than *T. jiufengensis*.

The palatine extends anteriorly to the level of the posterior margin of the tusks, and it distinctly decreases in width posteriorly (Fig. 1C, D). The posterior extension of the ectopterygoid is shorter than that of the palatine in ventral view (Fig. 1C, D). The interpterygoid vacuity is drop-shaped and expose the parabasisphenoid ventrally. It's margin is contributed by the vomer anteriorly and the pterygoid posteriorly.

The anterior pterygoid keel extends for the entire anterior ramus of the pterygoid (Fig. 1C, D), as in *T. jiufengensis* (Liu, 2021). The posterior portion of the keel of the anterior pterygoid ramus cannot be discerned, but in IVPP V3241, some trace can be observed of this portion (Fig. 2E). Only the anterior process of the epipterygoid is preserved on the left side, bordered by the pterygoid (Fig. 1E, F). The quadratojugal is plate-like. The quadrate has a rounded anterior edge, as in most dicynodonts (Fig. 1E, F). The periotic has a rod-like pila antotica. The sphenethmoid (“anterior plate”) complex consists of the orbitosphenoid and mesethmoid, but their sutures are unidentifiable (Fig. 1E, F).

**Mandible:** The mandible is nearly complete (Fig. 3), and its shape is nearly identical to that of *Turfanodon jiufengensis*. The symphysis is composed of the dentary, the splenial and the angular, and forms an upturned beak (Fig. 3). The anterior surface of the symphysis has a median ridge and two lateral ridges that follow the lateral edges (Fig. 3A, B). The symphysis and the mandibular rami form a narrow junction anterior to the lateral dentary shelf. This narrow portion could accommodate the enlarged caniniform processes when the jaw was closed (Fig. 3E). Dentary tables are present. The posterior dentary sulcus developed as a narrow groove with two sharp ridges bound it (Fig. 3E). The lateral dentary shelf is developed as a prominent swelling above the anterior margin of the mandibular fenestra, unlike the thin

shelf of *T. jiufengensis* (Fig. 3A, B). Its morphology is somewhat similar to that of *Kunpania*, but *Kunpania* has more distinct dorsal and ventral surfaces (Angielczyk et al., 2021b).

The ventral margin of the reflected lamina is incomplete. A thin ridge runs posterodorsally above the dorsal notch (Fig. 3A, B), without any expansion in its dorsal end, differing from the condition in *Jimusaria* (Shi and Liu, 2023). The posteroventral fossa is partly preserved on ventral margin of the reflected lamina. The angular gap is wide, and forms a distinct angular fossa (Fig. 3A, B).

**Postcranial skeleton: Vertebrae and ribs** At least 26 vertebrae are preserved, although many of them are preserved only as the amphicoelous centra (Fig. 4A–I). Three articulated dorsal vertebrae and three sacral vertebrae might belong to IVPP V31403, considering their smaller size (Fig. 4G, H). Only those vertebrae that can be referred to specific regions are described here (Fig. 4C–H).

The axis and the third cervical are articulated (Fig. 4A, B). The axis features an anteroposteriorly expanded neural spine and the odontoid. The prezygapophysis is broken but the postzygapophysis extends posteriorly beyond the posterior margin of the centrum. A small boss is developed near the anterior margin of axis centrum, posterior to the odontoid. King (1981) proposed that is a facet for a cervical rib in “*Dicynodon trigonocephalus*”, but the rib is not observed here or in the specimens of *T. jiufengensis* (Liu, 2021).

The dorsal vertebrae feature high, nearly vertical neural spines; reduced, more vertically oriented prezygapophyse; horizontally oriented postzygapophyses and slight overlap of the postzygapophyses by the prezygapophyses from the lateral side. Their lateral surfaces of the centra are slightly concave and smooth (Fig. 4C, D).

Three sacral vertebrae of IVPP V31402 can be identified, likely the first to the third. They are identified by the elongated and vertically oriented prezygapophyses of the second one and the third one, the reduced postzygapophyses, the posterodorsally oriented neural spine, and the fused centra and zygapophyses. The centrum of the third sacral of the series is anteroposteriorly elongate and laterally narrow (Fig. 4E). The third through fifth sacral

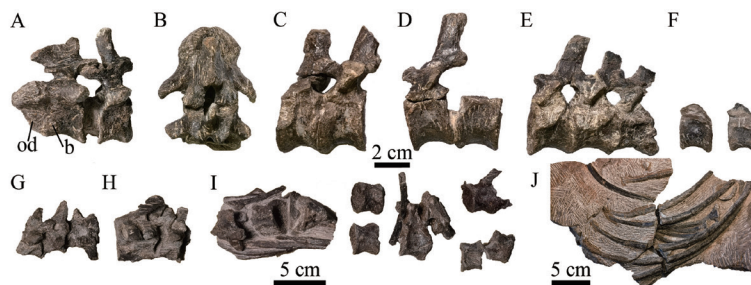


Fig. 4 *Turfanodon bogdaensis* from the Guodikeng Formation, Turpan, Xinjiang

A–F. IVPP V31402, axis and the third cervical in left lateral (A) and dorsal (B) views, four dorsal vertebrae (C, D), three (1st–3rd) sacral vertebrae (E), and two caudal vertebrae (F) in left lateral view; G–H. V31403, three dorsal vertebrae (G) in dorsal view and three (3rd–5th) sacral vertebrae (H) in left lateral view; I, J. unidentified vertebrae (I) and ribs (J). Abbreviations: b. boss; od. odontoid

vertebrae are preserved in V31403 (Fig. 4H). The fourth sacral vertebra still fused with the third one, and the base of its neural spine extends more posteriorly than the anterior one, as in *T. jiufengensis* (Liu, 2021). The fifth sacral vertebra does not fused with the fourth, and its prezygapophyses are reduced in size compared to those of the more anterior sacral vertebrae.

At least two caudal vertebrae are preserved, consisting of only centra and incomplete neural arches (Fig. 4F). They lack the transverse processes and rib facets.

Several separate ribs are preserved, most of them are only partially exposed from the surrounding matrix (Fig. 4J). One exposed proximal end is holocephalous and grooves are present on the shafts of some ribs, indicating those ribs belong to the posterior portion of the dorsal rib series.

**Sternum:** The incomplete sternum is preserved with the left pectoral girdle, and is exposed ventrally (Fig. 5A). It is parallelogram-shaped, measuring ~11 cm in anteroposterior length. One sternal boss present along the lateral margin (Fig. 5B).

**Pectoral girdle:** The preserved pectoral girdles include the scapula, procoracoid, and coracoid from the left side and the procoracoid and coracoid from the right side. The clavicles are missing. The left pectoral girdle is articulated (Fig. 5A, B), while the right one is separated (Fig. 5C, D).

The scapula is distinctly convex laterally, fitting the body contour (Fig. 5A, B). Its anterior edge projects laterally as a crest, and the origin of the *M. triceps scapularis* is developed as rugosity. The scapula has a large ventral articular surface for the procoracoid, and a deep notch on the ventral margin. This notch contributes to the border of the coracoid foramen (Fig. 5A, B). The acromion process is incomplete but well defined (Fig. 5A).

The procoracoid and coracoid are sutured together as the coracoid plate (Fig. 5B). The procoracoid is a nearly square bone with a notch on the posterodorsal edge (Fig. 5A–C). This notch forms the procoracoid portion of the coracoid foramen. The procoracoid does not participate in the glenoid (Fig. 5B). The coracoid has a strongly concave medial surface (Fig. 5B, D). The origin of the *triceps coracoideus* is thicker than the other portion of the

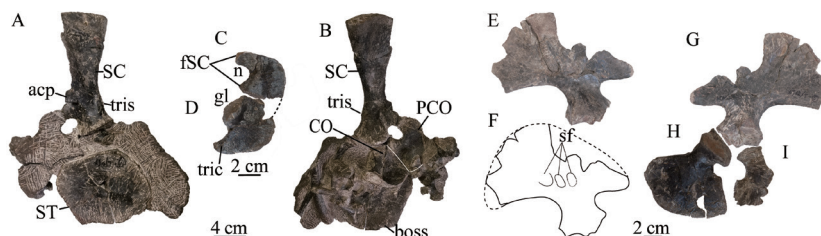


Fig. 5 *Turfanodon bogdaensis* (IVPP V31402) from the Guodikeng Formation, Turpan, Xinjiang  
A, B. left pectoral girdle in lateral (A) and medial (B) views; C, D. right procoracoid (C) and right coracoid (D)  
in lateral view; E–G. photos and drawing of right ilium in medial (E, F) and lateral (G) views;

H. right ischium in lateral view; I. mirrored left pubis in lateral view

Abbreviations: acp. acromion process; CO. coracoid; fSC. facet for scapula; gl. glenoid fossa on coracoid;  
n. notch; PCO. procoracoid; SC. scapula; sf. facet for sacral ribs; ST. sternum;  
tric. origin of *triceps coracoideus*; tris. origin of *triceps scapularis*

coracoid edge (Fig. 5D).

**Pelvic girdle:** The elements of the pelvic girdle are disarticulated. The ilia and the ischia of both sides are preserved, but the right ones are more complete; only the left pubis is preserved (Fig. 5E–I).

The dorsal edge of the iliac blade is incomplete (Fig. 5E–G). The preacetabular process is longer and higher than the postacetabular process. Medially, three facets for the sacral ribs can be observed on the middle (Fig. 5E, F). According to Liu (2021), *Turfanodon jiufengensis* possibly has six sacral ribs. The fossae of *T. bogdaensis* suggest that at least three ribs are firmly articulated with the ilium and the rest of them are free from it in this species. A constricted neck lies ventral to the blade.

The ischium is a fan-shaped plate, it contributes to the posterior portion of the acetabulum (Fig. 5H). The outer surface is slightly convex. A notch for the obturator foramen lies anterior to the neck of the ischium, close to the acetabulum.

The pubis is a relatively small bone (Fig. 5I). Its body is laterally curved, the posterior portion has a notch, which forms the anterior margin of the obturator foramen.

**Limbs:** Three humeri and two different sized femora are preserved together, indicating that there are at least two individuals preserved (Fig. 6). Based on the sizes of the articular facets of the limb girdles and proximal widths of the limbs, the larger limb bones are referred to the same individual as the limb girdles. The larger humerus is similar in size to a humerus of *T. jiufengensis* (IVPP V26035) (Fig. 6E, F), the skull of which is of comparable size with IVPP V31402 (Liu, 2021) (Fig. 2). Based on this, the larger limbs and girdles are referred to the same individual as the cranial material here.

**Forelimb:** The humeri are well-preserved, including two larger both side humeri (IVPP V31402, Fig. 6A, B, E), and a smaller complete right humerus (V31403, Fig. 6C). Dorsally, the humerus proximal head is rounded, and a rounded, rugose region lies posterior to the condyle, which is the insertion of the M. subscapularis (Fig. 6B). A bulge developed anterior to the humerus proximal head, which should be the insertion of the supracoracoideus (supraspinatus) (Ray, 2006; Bishop and Pierce, 2023a), but it is less developed in *Lystrosaurus* (Fig. 2C, D). A thin, curved deltopectoral crest is located anteroventral to the proximal head. This crest is a triangular, thin plate that is convex dorsally, and extends for nearly half the length of the humerus (Fig. 6A–C). The insertion of the M. latissimus dorsi (the insertion of the M. teres major according to Bishop and Pierce (2023a)) shows a pinna-like shape (Fig. 6A). The entepicondylar foramen penetrates the ridge which is elongated by the deltopectoral crest edge (Fig. 6B). The anteroposteriorly continuous distal articular facet, can be divided, from anterior to posterior, as the ectepicondyle, the ulnar condyle and the entepicondyle (Fig. 6E). Contra Kammerer (2018), a “supinator process” (the “brachioradialis process” according to Bishop and Pierce (2023a)) is present in *Turfanodon bogdaensis*, *T. jiufengensis* and even *Lystrosaurus* (Fig. 6A, D), located proximal to the ectepicondyle, and close to the base of the shaft as in the Triassic stahleckeriids *Pentasaurus* and *Zambiasaurus* (Kammerer, 2018).



Fig. 6 The limb bones of *Turfanodon*

A–C. right humerus of *T. bogdaensis* in dorsal (A, C) and ventral (B) views, IVPP V31402 (A, B), V31403 (C);

D. right humerus of *T. jiu Fengensis* in anterior view, V26035; E, F. comparison of right humerus of *T. bogdaensis* (V31402) (E) and *T. jiu Fengensis* (V26035) (F) in distal view; G, H. ulna (G) and radius (H) of *T. bogdaensis* (V31402) in anterior view; I–K. left (V31402) and right (V31403) femur of *T. bogdaensis* in dorsal (I) and ventral (J, K) views; L, M. tibia (L) and fibula (M) of *T. bogdaensis* (V31402) in anterior (L) and lateral (M) views; N, O. astragalus (N) and metatarsal (O) of *T. bogdaensis* (V31402)

Abbreviations: dep. deltopectoral crest; ec. ectepicondyle; en. entepicondyle; enf. entepicondylar foramen; fR. facet for radius; if. insertion of iliofemoralis; ld. insertion of latissimus dorsi (teres major); oc. olecranon process; ssc. insertion of subscapularis; sup. supinator (brachioradialis) process; trc. trochanteric crest; uc. ulna condyle

The ulna is incomplete, only the proximal portion is preserved. The proximal end is relatively flat and extends lateromedially (Fig. 6G). There is a triangular facet for the radius facing anteromedially. The proximal end extends laterally as a small olecranon process (Fig. 6G). The radius is a rod-like bone with a concave proximal end and a convex distal end (Fig. 6H).

**Hindlimb:** The preserved two femurs are slightly different in size but nearly identical in shape (Fig. 6I–K). The femur has a hemispherical head which is continuous with the shaft. Lateral to the femoral head is the trochanter major, which is a flat, broad crest. Distally, it bears the insertion of the M. iliofemoralis and the distal end convex anteriorly. The trochanteric crest is about 2/5 length of the femur; this ratio is larger than that of *Lystrosaurus* but similar to that

of the kannemeyeriiforms *Parakannemeyeria* and *Shanbeikannemeyeria* (Sun, 1963).

The left tibia and fibula are well preserved (Fig. 6L, M). The tibia is a robust bone with a prominently expanded proximal end and gently expanded distal end. The fibula is a thin, rod-like bone without any crest on the shaft. Medially, the proximal end of the tibia has a notch fitting the lateral condyle of the fibula. The proximal facet for femur of the fibula shows a “quotation mark” shape.

An astragalus (Fig. 6N) and metatarsal (Fig. 6O) are preserved. The astragalus is a nearly rounded bone, a groove and a concave developed on its surface.

#### 4 Discussion

IVPP V31402 can be referred to *Turfanodon* based on the combination of a narrow intertemporal bar, large temporal fenestra, premaxilla contacting the frontal, and nasals separated by the premaxilla and the frontal. A ‘three-toe’-shaped, depressed preparietal was previously proposed as an autapomorphy of *T. jiufengensis* (Liu, 2021). Although the preparietal of V31402 is ‘three-toe’-shape rather than oval, it can be referred to *T. bogdaensis* based on the presence of slightly raised nasal bosses, prefrontal anterior extension not extending anterior to lacrimal, and maxillary contact with nasal, indicating that preparietal shape does not allow confident distinction between the two species of *Turfanodon*.

We found more differences between *T. bogdaensis* and *T. jiufengensis*, including that the lateral surface of the snout region is nearly flat rather than concave (Fig. 2) and the lateral dentary shelf forms a prominent swelling rather than a thin sheet in *T. bogdaensis*. *T. bogdaensis* (IVPP V31402) has a more rounded femoral head, while *T. jiufengensis* (V26038) has a less distinct femoral head, although the latter is larger (and thus one would presume it would be better ossified) than V31402.

Within *T. bogdaensis*, different specimens exhibit different degrees of parietal exposure. IVPP V3241 and IGCAGS V296 have deep grooves overlapped by the parietals, but in IVPP V31402 the groove is relatively shallow, and is limited on the posterior portion of the intertemporal bar (Fig. 1A). This difference could be due to the ontogenetic variation. The narrowing of the intertemporal bar and the parietal exposure is a common ontogenetic variation among the dicynodonts (Kammerer et al., 2015).

This study presents the osteology of the mandible and postcranial skeleton of *Turfanodon bogdaensis*, including characters that were previously unknown for this genus. The postcranial bones are generally similar to those of other *Dicynodon*-grade dicynodontoids except for the shape of the ventral margin of the scapula: its basal portion is deeply notched by the large coracoid foramen and it appears there is a distinct anteroventral projection below the acromion process (Fig. 5A, B). A scapular contribution to the coracoid foramen is also present in, e.g., *Diictodon*, *Dicynodontoides*, *Lystrosaurus*, and *Ischigualastia*, but the scapulae in those taxa do not have such a deep notch as in IVPP V31402 (Young, 1935; Cox, 1959; Cox and

Parrington, 1965; Ray and Chinsamy, 2003; Angielczyk, 2007). This suggests that the deeply notched scapula is autapomorphic for the genus *Turfanodon*. The large coracoid foramen might house a robust subclavian artery passing through (Romer, 1956). The insertion of the M. supracoracoideus is strongly developed on the humerus (Fig. 2C), indicating that this muscle was well-developed in *Turfanodon*. Both the more abundant blood supply and strong M. supracoracoideus suggest well-developed anterodorsal movement of the forelimb (Ray and Chinsamy, 2003; Ray, 2006; Bishop and Pierce, 2023a).

Variation in the preparietal: Referral of IVPP V31402 to *Turfanodon bogdaensis* indicates that the “three-toe” shaped preparietal is not exclusive to *T. jiufengensis*, and the preparietal shape shows substantial variation in *T. bogdaensis* specimens. Because the oval-shaped preparietal appears in relatively larger skulls, this variation may be related ontogeny. In *T. jiufengensis*, the preparietal shape is unknown in the large skull, but it shows some variation in the small-sized skulls (Liu, 2021). Based on the condition in *T. bogdaensis*, we now hypothesize that *T. jiufengensis* also had an oval-shaped preparietal in the adult.

Two other dicynodont specimens show the similar preparietal shape to that of small *Turfanodon*: NHMUK R4955 and RC 64. NHMUK R4955 is the holotype of *Palemydops platysoma* and has a trident-shaped preparietal with anterior and lateral processes of comparable length, plus a unique posterior elongation of the pineal foramen (Broom, 1921; Boos et al., 2016). RC 64 is the holotype of *Dicynodon duvenhagei*, in which the preparietal has three similar processes, but the suture is more tortuous than in *Turfanodon* (Broom, 1947). The validity of both species is questionable. NHMUK R4955 was considered a possible specimen of *Pristerodon mackayi*, but later regarded as a nomen dubium due to its incomplete preparation by Keyser (1993), although King (1988) considered it valid but of uncertain relationships. RC 64 was referred to *Kingoria* by Cluver and Hotton (1981), and subsequently referred to the species *Dicynodontoides recurvidens* (Angielczyk et al., 2009; Kammerer et al., 2011). A preparietal with three processes is unknown in the other published specimens of *Dicynodontoides*, and is also rare within Bidentalia.

**Acknowledgements** We thank LI Lu, LIU Yu-Feng, LI Xing-Wen, and XU Xu for the fieldwork, GAO Wei for the photograph, XU Yong for optimizing drawings. We also thank Christian Kammerer and Kenneth Angielczyk, their comments and edit improved this article. This work is supported by Strategic Priority Research Program of Chinese Academy of Sciences (XDB26000000) and The Innovation Training Programs for Undergraduates, Chinese Academy of Sciences.

## 博格达吐鲁番兽(二齿兽类)的骨骼学

石雨泰<sup>1,2</sup> 刘俊<sup>1,2</sup>

(1 中国科学院古脊椎动物与古人类研究所, 中国科学院脊椎动物演化与人类起源重点实验室 北京 100044)

(2 中国科学院大学地球与行星科学学院 北京 100049)

**摘要:** 吐鲁番兽(*Turfanodon*)是一类生活在二叠纪晚期的二齿兽类, 曾广泛分布在新疆至华北一带。目前该属下建立有两个种——博格达种(*T. bogdaensis*)与九峰种(*T. jiufengensis*)。两个种都具有相对完整的头骨材料, 但只有九峰种报道了下颌及头后骨骼材料。一批产自新疆吐鲁番地区, 可以归入到博格达吐鲁番兽的新材料, 具有一系列可以明显区别于九峰种的特征, 包括头骨的鼻吻部侧面平坦, 下颌齿骨侧架成肿突状, 以及股骨头为近半球状。吐鲁番兽属的鉴别特征也有更新, 包括眼框周缘平坦, 两条翼骨前支上的嵴向后汇聚, 以及一个可能的自有衍征: 肩胛骨上参与塑造乌喙孔的凹缺很大。吐鲁番兽髂部的中嵴两侧发育有副嵴。这一特征区别于除肌龙兽(*Myosaurus*)、掘铁兽(*Kembawacela*)和水龙兽(*Lystrosaurus*)外的其他二齿兽类。

**关键词:** 新疆吐鲁番盆地, 二叠纪乐平世, 锅底坑组, 二齿兽类, 吐鲁番兽, 骨骼学, 头后骨骼

### References

- Angielczyk K D, 2007. New specimens of the Tanzanian dicynodont “*Cryptocynodon*” *parringtoni* von Huene, 1942 (Therapsida, Anomodontia), with an expanded analysis of Permian dicynodont phylogeny. *J Vert Paleontol*, 27(1): 116–131
- Angielczyk K D, Sidor C A, Nesbitt S J et al., 2009. Taxonomic revision and new observations on the postcranial skeleton, biogeography, and biostratigraphy of the dicynodont genus *Dicynodontoides*, the senior subjective synonym of *Kingoria* (Therapsida, Anomodontia). *J Vert Paleontol*, 29(4): 1174–1187
- Angielczyk K D, Benoit J, Rubidge B S et al., 2021a. A new tusked cistecephalid dicynodont (Therapsida, Anomodontia) from the upper Permian upper Madumabisa Mudstone Formation, Luangwa Basin, Zambia. *Pap Palaeontol*, 7(1): 405–446
- Angielczyk K D, Liu J, Yang W, 2021b. A redescription of *Kunpania scopulosa*, a bidentalid dicynodont (Therapsida, Anomodontia) from the ?Guadalupian of northwestern China. *J Vert Paleontol*, 41(1): e1922428
- Angielczyk K D, Liu J, Sidor C A et al., 2022. The stratigraphic and geographic occurrences of Permo-Triassic tetrapods in the Bogda Mountains, NW China—implications of a new cyclostratigraphic framework and Bayesian age model. *J Afr Earth Sci*, 195: 104655
- Bishop P J, Pierce S E, 2023a. The fossil record of appendicular muscle evolution in Synapsida on the line to mammals: Part I—Forelimb. *Anat Rec*, 1–62

- Bishop P J, Pierce S E, 2023b. The fossil record of appendicular muscle evolution in Synapsida on the line to mammals: Part II—Hindlimb. *Anat Rec*, 1–71
- Boos A D, Kammerer C F, Schultz C L et al., 2016. A new dicynodont (Therapsida: Anomodontia) from the Permian of southern Brazil and its implications for Bidentalian origins. *PLoS One*, 11(5): e0155000
- Broom R, 1921. 35. On some new genera and species of anomodont reptiles from the Karroo Beds of South Africa. *Proc Zool Soc Lond*, 91(4): 647–674
- Broom R, 1947. XXI.—A contribution to our knowledge of the vertebrates of the Karroo Beds of South Africa. *Trans R Soc Edinb*, 61(2): 577–629
- Chen J, Liu J, 2022. A late Permian archosauriform from Xinjiang shows evidence of parasagittal posture. *Sci Nat*, 110(1): 1
- Cluver M A, 1971. The cranial morphology of the dicynodont genus *Lystrosaurus*. *Ann S Afr Mus*, 56(5): 155–274
- Cluver M A, 1974. The cranial morphology of the Lower Triassic dicynodont *Myosaurus gracilis*. *Ann S Afr Mus*, 66: 35–54
- Cluver M A, Hooton N, III, 1981. The genera *Dicynodon* and *Diictodon* and their bearing on the classification of the Dicynodontia (Reptilia, Therapsida). *Ann S Afr Mus*, 83(6): 99–146
- Cox C B, 1959. On the anatomy of a new dicynodont genus with evidence of the position of the tympanum. *Proc Zool Soc Lond*, 132(3): 321–367
- Cox C B, Parrington F R, 1965. New Triassic dicynodonts from South America, their origins and relationships. *Philos Trans R Soc Lond, Ser B*, 248: 457–514
- Kammerer C F, 2018. The first skeletal evidence of a dicynodont from the lower Elliot Formation of South Africa. *Palaeontol Afr*, 52: 102–128
- Kammerer C F, Angielczyk K D, Fröbisch J, 2011. A comprehensive taxonomic revision of *Dicynodon* (Therapsida, Anomodontia) and its implications for dicynodont phylogeny, biogeography, and biostratigraphy. *J Vert Paleontol*, 31(sup1): 1–158
- Kammerer C F, Angielczyk K D, Fröbisch J, 2015. Redescription of the geikiid *Pelanomodon* (Therapsida, Dicynodontia), with a reconsideration of ‘*Propelanomodon*’. *J Vert Paleontol*, 36 (1): e1030408
- Keyser A W, 1993. A re-evaluation of the smaller endothiodontidae. Pretoria: Government Printer. 1–53
- King G M, 1981. The functional anatomy of a Permian dicynodont. *Philos Trans R Soc Lond—Biol Sci*, 291: 244–322
- King G M, 1988. Anomodontia. Stuttgart: Gustav Fischer Verlag. 1–174
- Li P X, Cheng Z W, Li J L, 2000. A new species of *Dicynodon* from Upper Permian of Sunan, Gansu, with remarks on related strata. *Vert Palasiat*, 38(2): 147–157
- Liu J, 2021. The tetrapod fauna of the upper Permian Naobaogou Formation of China: 6. *Turfanodon jiufengensis* sp. nov. (Dicynodontia). *PeerJ*, 9: e10854
- Olroyd S L, Sidor C A, 2022. Nomenclature, comparative anatomy, and evolution of the reflected lamina of the angular in non-mammalian synapsids. *J Vert Paleontol*, 42(1): e2101923
- Olson E C, 1944. Origin of mammals based upon cranial morphology of the therapsid suborders. *Spec Pap, Geol Soc Am*, 55: 1–136
- Owen R, 1859. On some reptilian remains from South Africa. *Edinb N Philos J*, 10 new series: 289–291
- Owen R, 1860. On the orders of fossil and recent Reptilia, and their distribution in time. Report of the Twenty-Ninth Meeting

- of the British Association for the Advancement of Science. London: The British Association for the Advancement of Science. 153–166
- Ray S, 2006. Functional and evolutionary aspects of the postcranial anatomy of dicynodonts (synapsida, Therapsida). *Palaeontology*, 49(6): 1263–1286
- Ray S, Chinsamy A, 2003. Functional aspects of the postcranial anatomy of the Permian dicynodont *Diictodon* and their ecological implications. *Palaeontology*, 46(1): 151–183
- Romer A S, 1956. *Osteology of the Reptiles*. Chicago: University of Chicago Press. 1–772
- Shi Y T, Liu J, 2023. The tetrapod fauna of the upper Permian Naobaogou Formation of China: 10. *Jimusaria monanensis* sp. nov. (Dicynodontia) shows a unique epipterygoid. *PeerJ*, 11: e15783
- Sun A L, 1963. The Chinese kannemeyeriids. *Palaeontol Sin, New Ser C*, 17: 1–109
- Sun A L, 1973. Permo-Triassic dicynodonts from Turfan, Sinkiang. *Mem Inst Vert Paleont Paleoanthrop, Acad Sin*, 10: 53–68
- Sun A L, 1978. Two new genera of Dicynodontidae. *Mem Inst Vert Paleont Paleoanthrop, Acad Sin*, 13: 19–25
- Young C C, 1935. On two skeletons of Dicynodontia from Sinkiang. *Bull Geol Surv China*, 14(4): 483–518